Int. Journal of Refractory Metals and Hard Materials 50 (2015) 253–257

Contents lists available at ScienceDirect

Int. Journal of Refractory Metals and Hard Materials

journal homepage: www.elsevier.com/locate/IJRMHM

Development of tungsten-based materials by different sintering techniques

Kameel Arshad [a], Jun Wang [a], Yue Yuan [a,*], Ying Zhang [a], Zhang-Jian Zhou [b], Guang-Hong Lu [a]

[a] School of Physics and Nuclear Energy Engineering, Beihang University, Beijing 100191, China
[b] School of Materials Science and Engineering, University of Science and Technology Beijing (USTB), Beijing 100083, China

ARTICLE INFO

Article history:
Received 8 December 2014
Received in revised form 2 February 2015
Accepted 3 February 2015
Available online 7 February 2015

Keywords:
Tungsten vanadium composites
Sintering techniques
Microstructures
Mechanical properties

ABSTRACT

The effects of different sintering techniques on the densification, microstructure, and mechanical properties of tungsten–vanadium composites were investigated. The precursor powders were conventionally mixed with a combination of W–5 wt.%V in a blender and then sintered by three different sintering techniques. A good dense sample with the lowest porosity, and the highest bending strength and micro-hardness was obtained by hot-press sintering, reached up to 3.5%, 508.9 MPa and 589.8 $HV_{0.2}$, respectively. Spark plasma sintering was beneficial to obtain more refined tungsten grains as compared to hot-press sintering and conventional sintering under hydrogen atmosphere. However, the insufficient sintering conditions of spark plasma sintering were not able to highly suppress the porosity, and thus the mechanical properties were inadequate in comparison with hot press sintering. The properties measured for hydrogen furnace sintered sample were very poor in all respects.

1. Introduction

Tungsten (W) due to its attractive properties, such as high melting point, low sputtering yield, high thermal conductivity and low thermal expansion coefficient is considered as a promising candidate material for high temperature applications [1]. However, a major drawback for its use is the inherent high ductile-brittle transition temperature (DBTT), poor ductility and low fracture toughness, recrystallization brittleness and radiation induced brittleness [2]. Fine-grained W materials have shown attractive properties in terms of reduction in brittleness and improvement in toughness and strength [1,3]. However, the mechanical properties of these materials at higher temperatures (higher than the recrystallization temperature) for long time are highly deteriorated.

Fabrication techniques influence the densification, microstructures and all related properties of the sintered metals [4,5]. The grain growth usually occurs at the peak sintering temperature where the temperature and dwell time are highest [4]. In hot pressing (HP) and spark plasma sintering (SPS), a uniaxial pressure is applied to densify the sintered sample [6,7]. Thus in comparison with conventional sintering in hydrogen furnace (HF), relatively low sintering temperature and short dwell time are required for HP and SPS which thereby inhibit the grain growth during sintering [4,8].

Due to the high melting point of W, full densification of W-based materials is rather difficult to be obtained by sintering. Post-processes (e.g. hot rolling, subsequent repressing, resintering and hot isostatic pressing) are occasionally used to improve the density [9,10]. However, these post-processes meanwhile affect the microstructures (e.g. recrystallization and grain growth) and mechanical properties of targeted materials [11]. An alternative approach is the addition of small amounts of doping elements, such as V, Ti, Y, La_2O_3, and Y_2O_3, to activate sintering of W powder and thus to achieve good density [12–15]. Our recent studies suggest that the addition of V in W constrains the grain growth and improves the densification and mechanical properties [12,16]. V addition enhances the thermal stability of the microstructures and mechanical properties of W-based materials [17]. Moreover, V shows high stability against the activation and transmutation under neutron irradiation as compared to W, Re, Ta etc. [18].

In this study, we used different sintering techniques, including HP, SPS and HF, to produce W–V composites and investigated the effects of these techniques on the consolidation behavior, microstructures and mechanical properties of W–V composites. In this context, we expect to obtain a better sintering method for the development of W-based materials.

2. Experimental procedure

W and V powders of purity >99.9% with an average particle size of 2 μm and 0.8 μm respectively, were conventionally mixed with W–5wt.%V combination in a blender for 8 h. For HP, W–V powder was loaded into a graphite mold with a 35×30 mm^2 inner space and then heated to a peak temperature of 1800 °C. An axial pressure of 20 MPa was applied on the sample after 1100 °C. The furnace was switched off immediately after sintering at 1800 °C for 2 h and the sample was cooled down under vacuum. For SPS, the mixed powder was loaded into a

* Corresponding author.
E-mail address: yueyuan@buaa.edu.cn (Y. Yuan).

http://dx.doi.org/10.1016/j.ijrmhm.2015.02.004
0263-4368/

graphite mold with an inner diameter of 20 mm. The sample was then sintered by SPS at 1600 °C for 3 min in vacuum. The sintering temperature and dwell time were selected according to the maximum capability of SPS device. An axial pressure of 20 MPa was applied on the sample at the start and then increased to 50 MPa above 1500 °C. For HF, the mixed powder was initially compacted by cold isostatic pressing and then sintered by the HF technique. The heat rate, sintering temperature and dwell time for HF were the same as HP, with the only difference that no pressure was applied on the sample during sintering in the case of HF.

The morphology of cracked and polished surfaces of the sintered samples was characterized by scanning electron microscopy (SEM). The porosity level of different sintered W–V materials was estimated from the measured density by the Archimedes' method and the theoretical calculated density [16]. Vicker's micro-hardness values of well polished bulk samples were measured at room temperature by applying a load of 1.96 N for 10 s. The micro-hardness value of each sample was determined by averaging 8–10 different indents. A well polished $2 \times 3 \times 18$ mm^3 specimen of each sintered material with a span of 13.1 mm was subjected to a three point bending test with a cross head speed of 0.5 mm/min at room temperature.

3. Results and discussion

The SEM images along with elemental map distribution of polished surfaces of W–V samples consolidated by different techniques (HP, SPS and HF), named as S_{HP}, S_{SPS} and S_{HF} respectively, are illustrated in Fig. 1(a–c). The respective quantitative energy-dispersive X-ray spectroscopy (EDS) analysis of S_{HP}, S_{SPS} and S_{HF} samples is presented in Fig. 1(d–f). The EDS mapping of S_{HP} (Fig. 1(a)), demonstrates that dark gray regions as pointed out by a red arrow are W–V alloy zones and the alloying formation and mutual diffusion of W and V took place during HP sintering process. Fig. 1(d) shows that the EDS analysis of the part of dark gray region as marked by cross (yellow color) also confirms a large peak of W in V enrich zone which further proves the alloying formation for S_{HP}. Moreover, few small pores are found as pointed out by a white arrow. The SEM image along with its EDS mapping of S_{SPS} as shown in Fig. 1(b) reveals that the V-enriched phases are unevenly distributed in W matrix (indicated by a red arrow) and small white spots are pores (indicated by a white arrow). The EDS analysis of S_{SPS} as shown in Fig. 1(e) demonstrates that the large dark black regions on polished surface are V-enriched phases and almost no alloying formation took place during SPS, as a very small W peak is detected in that region. Similar results of EDS analysis of the milled SPS sintered samples can also be found in our article [16]. The phenomenon of alloying formation during SPS consolidation is not obvious due to its relatively low sintering temperature and short dwell time [16]. Fig. 1(c) clearly illustrates large size pores with irregular shapes on the polished surface of S_{HF} as pointed by a white arrow, due to the disadvantage of pressureless sintering and dark V-enriched phase unevenly distributed similar to S_{SPS} up to some extent, as pointed by a red arrow. The alloying formation is also not observed for S_{HF} as indicated by EDS analysis (Fig. 1(f)).

Fig. 2 shows the fracture surfaces of S_{HP}, S_{SPS} and S_{HF} respectively. The comparative SEM analyses reveal that S_{HP} (Fig. 2(a)) is highly compacted and has the lowest porosity as also shown in Fig. 1(a). Although the cracking pattern exhibits mix cracking, it is mainly transgranular and it is expected to have high mechanical strength. The

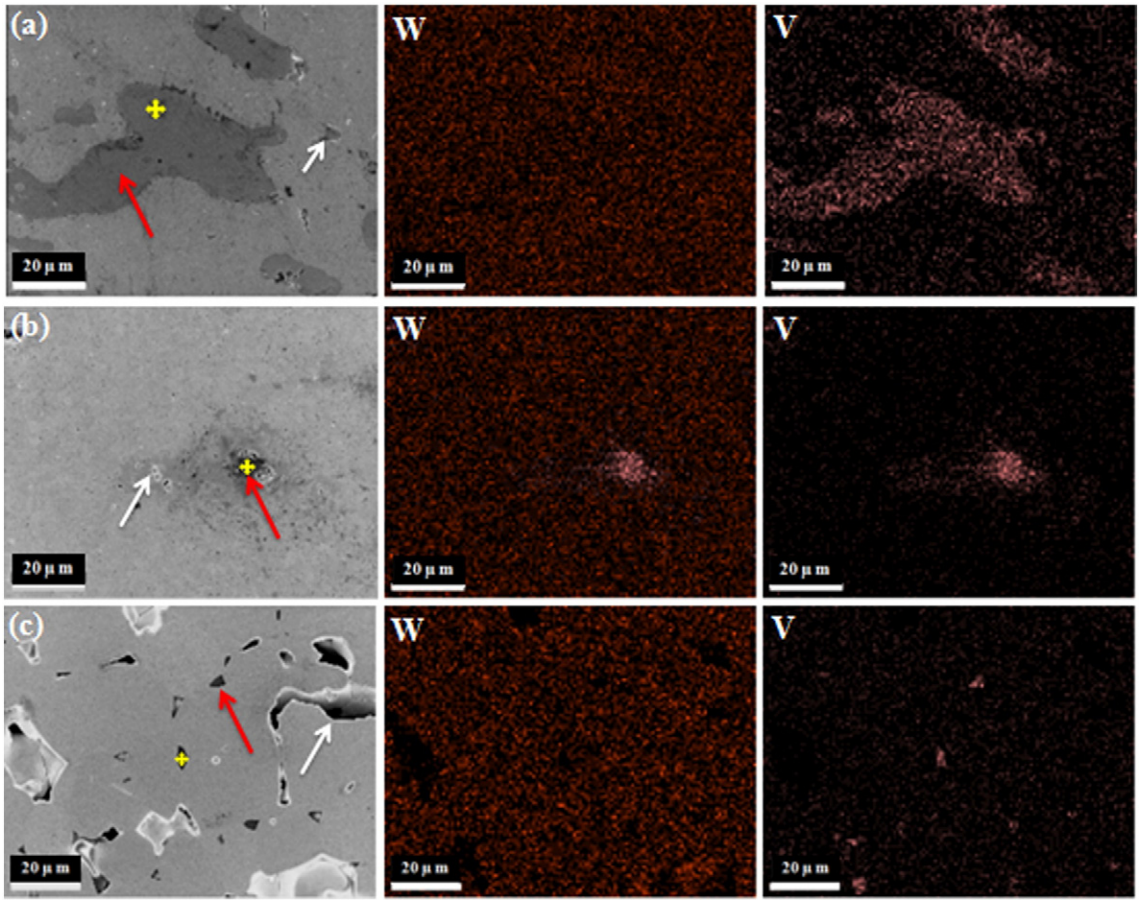

Fig. 1. The elemental map distribution of the mirror polished surface: (a) S_{HP}, (b) S_{SPS}, and (c) S_{HF}, and the white and red arrows represent pores and V-enriched phases, respectively. EDS analysis of the small region pointed by yellow cross for different samples: (d) S_{HP}, (e) S_{SPS}, and (f) S_{HF}, respectively.